

Towards Robust Reasoning over Knowledge Graphs

Zhaohan Xi[†] Ren Pang[†] Changjiang Li[†] Shouling Ji[‡] Xiapu Luo^{*} Xusheng Xiao[§] Ting Wang[†]
[†]Pennsylvania State University ^{*}The Hong Kong Polytechnic University
[‡]Zhejiang University and Ant Financial [§]Case Western Reserve University

Abstract

Answering complex logical queries over large-scale knowledge graphs (KGs) represents an important artificial intelligence task, entailing a range of applications. Recently, knowledge representation learning (KRL) has emerged as the state-of-the-art approach, wherein KG entities and the query are embedded into a latent space such that entities that answer the query are embedded close to the query. Yet, despite its surging popularity, the potential security risks of KRL are largely unexplored, which is concerning, given the increasing use of such capabilities in security-critical domains (e.g., cyber-security and healthcare).

This work represents a solid initial step towards bridging this gap. We systematize the potential security threats to KRL according to the underlying attack vectors (e.g., knowledge poisoning and query perturbation) and the adversary’s background knowledge. More importantly, we present ROAR¹, a new class of attacks that instantiate a variety of such threats. We demonstrate the practicality of ROAR in two representative use cases (i.e., cyber-threat hunting and drug repurposing). For instance, ROAR attains over 99% attack success rate in misleading the threat intelligence engine to give pre-defined answers for target queries, yet without any impact on non-target ones. Further, we discuss potential countermeasures against ROAR, including filtering of poisoning facts and robust training with adversarial queries, which leads to several promising research directions.

1 Introduction

A knowledge graph (KG) is a structured representation of human knowledge about “facts”, with entities, relations, and descriptions respectively capturing real-world objects (or abstract concepts), their relationships, and their semantic properties. Answering complex logical queries over KGs represents an important artificial intelligence task, entailing a range of applications. For instance, in Figure 1, the security analyst queries for the most likely vulnerability (CVE) that is being exploited, based on observations regarding the incident (e.g., attack technique, tactics, and affected product).

Typically, the computational complexity of processing such queries grows exponentially with the query size [19], which

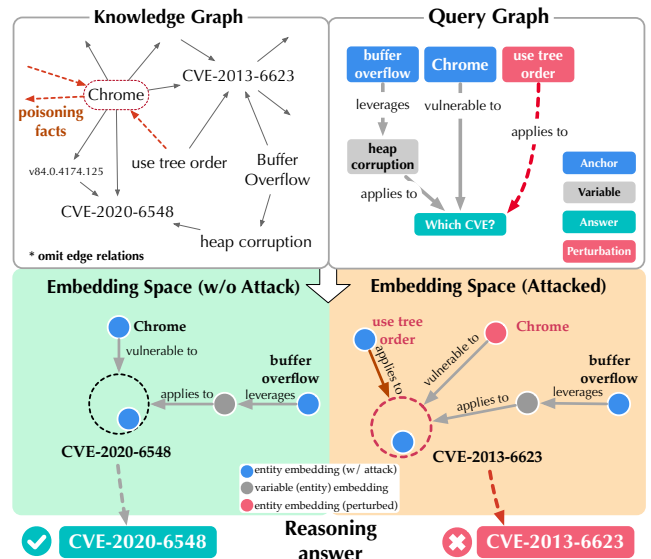


Figure 1: Illustration of KRL.

hinders its use over large KGs. Recently, *knowledge representation learning* (KRL) has emerged as a promising approach, wherein KG entities and a query are projected into a latent space such that the entities that answer the query are embedded close to each other. As shown in Figure 1, KRL reduces answering an arbitrary query to simply identifying entities with embeddings most similar to the query, thereby implicitly imputing missing relations [12] and scaling up to large-scale KGs in various domains [2, 3, 5].

Surprisingly, in contrast to the intensive research on improving the capabilities of KRL, its security risks are largely unexplored. This is highly concerning given (i) the importance of integrating domain knowledge in artificial intelligence tasks has been widely recognized [40]; (ii) KGs have emerged as one of the most popular representations of domain knowledge in various security-sensitive domains (e.g., cyber-security [30] and healthcare [50]); and (iii) KRL has become the state-of-the-art approach to process complex queries over such KGs [19, 38]. We thus wonder:

RQ₁ – What are the potential security threats to KRL?

RQ₂ – How effective are the attacks in practical settings?

RQ₃ – Are there any countermeasures against such attacks?

Our work – This work represents a solid initial step towards answering these questions.

RA₁ – First, we characterize the potential security threats

¹ROAR: Reasoning Over Adversarial Representations.

to KRL. As illustrated in Figure 1, the adversary may disrupt the reasoning of KRL through two attack vectors: (i) knowledge poisoning – polluting the KGs by committing poisoning facts, and (ii) query perturbation – modifying the queries by adding misleading variables/relations. We create a threat taxonomy according to the underlying attack vectors as well as the adversary’s background knowledge.

RA₂ – Further, we present ROAR, a new class of attacks that instantiate the above threats. We evaluate the practicality of ROAR attacks in two representative use cases, cyber-threat hunting and drug repurposing. It is empirically demonstrated that ROAR is highly effective against the state-of-the-art KRL systems in both domains. For instance, in both cases, ROAR attains over 99% attack success rates in misleading KRL to give pre-defined answers for target queries, yet without any impact on non-target queries.

RA₃ - Finally, we discuss potential countermeasures and their technical challenges. According to the attack vectors, we consider two mitigation strategies: (i) filtering of poisoning KG facts and (ii) robust training with adversarial queries. We reveal that there exists an interesting synergy between the two defenses and also a delicate trade-off between KRL performance and attack resilience.

Contributions – To the best of our knowledge, the work represents the first in-depth study on the security of KRL. Our contributions are summarized as follows.

We characterize the potential security threats to KRL and reveal the design spectrum for the adversary with varying capability and knowledge.

We present ROAR, a new class of attacks that instantiate various threats to KRL, which highlights with the following features: (i) it leverages both knowledge poisoning and query perturbation as the attack vectors; (ii) it is highly effective and evasive; (iii) it assumes limited knowledge regarding the target KRL system; and (iv) it realizes both targeted and untargeted attacks.

We discuss potential mitigation, which sheds light on improving the current practice of training and using KRL, pointing to several promising research directions.

2 Preliminaries

We first introduce fundamental concepts and assumptions used throughout the paper.

Knowledge Graph – A knowledge graph (KG) $\mathcal{G} = (\mathcal{N}, \mathcal{E})$ consists of nodes \mathcal{N} and edges \mathcal{E} connecting them. Each node $v \in \mathcal{N}$ represents an entity and each edge $v \xrightarrow{r} v' \in \mathcal{E}$ indicates that there exists relation $r \in \mathcal{R}$ (where \mathcal{R} is a finite set of relation types) from v to v' . In other words, \mathcal{G} comprises a set of facts $\{v, r, v'\}$ with $v, v' \in \mathcal{N}$ and $v \xrightarrow{r} v' \in \mathcal{E}$.

Query – A variety of reasoning tasks can be performed over KGs. Here, we focus on two types of queries.

Entity Query – In an entity query, one asks for a specific entity that satisfies given logical constraints, which are often defined using first-order conjunctive logic with existential (\exists) and conjunction (\wedge) operations. Formally, letting $v_?$ be the entity of interest, \mathcal{K}_q be the set of known *anchors*, \mathcal{V}_q be a set of existentially quantified *variables*, and \mathcal{E}_q be a set of relations, an entity query $q \triangleq (v_?, \mathcal{K}_q, \mathcal{V}_q, \mathcal{E}_q)$ is defined as:

$$q[v_?] = v_?. \exists \mathcal{V}_q : \bigwedge_{v \xrightarrow{r} v' \in \mathcal{E}_q} v \xrightarrow{r} v' \\ \text{s.t. } v \xrightarrow{r} v' = \begin{cases} v \in \mathcal{K}_q, v' \in \mathcal{V}_q \cup \{v_?\}, r \in \mathcal{R} \\ v, v' \in \mathcal{V}_q \cup \{v_?\}, r \in \mathcal{R} \end{cases} \quad (1)$$

As an example, in Figure 1, $v_?$ is the sink (CVE), Chrome is an anchor, while heap corruption is a variable.

Intuitively, q can be represented as a *dependency graph*, of which the nodes and edges correspond to the entities and relations in q , respectively. We say that a query q is valid if its dependency graph is directed acyclic with \mathcal{K}_q as the source nodes and $v_?$ as the unique sink node [19, 38].

Relation Query – In a relation query, one asks for the potential relation, which is currently not present in the KG, between two given entities v, v' . Formally, a relation query $q \triangleq (r_?, v, v')$ is defined as:

$$q[r_?] = r_?. \exists v \xrightarrow{r_?} v' \quad (2)$$

To determine $r_?$, it often requires to account for the context surrounding v and v' in the KG.

Knowledge Representation Learning – Recently, knowledge representation learning (KRL) has emerged as the state-of-the-art approach to process such queries. It projects KGs and query q to a latent space, such that entities that answer q are embedded close to q .

As shown in Figure 2, a KRL system γ typically comprises two components, *encoder* ϕ that projects entity v to its embedding ϕ_v , and relation r -specific *operator* ψ_r that performs geometric transformation to ϕ_v to compute entities with relation r to v . KRL often samples a set of query-answer pairs from the KG as the training set and trains ϕ and ψ in a supervised manner.

Entity Query – To process entity query q , one may derive q ’s *computation graph* from its dependency graph with a set of operators: (i) projection - given entity set \mathcal{S} , it computes the entities with relation r to \mathcal{S} ; (ii) intersection - given a set of entity sets $\{\mathcal{S}_1, \mathcal{S}_2, \dots, \mathcal{S}_n\}$, it computes $\bigcap_{i=1}^n \mathcal{S}_i$. Intuitively, the computation graph specifies the procedure to answer q as traversing the KG: starting from the anchors, it iteratively applies the two operators, until reaching the unique sink [17].

Relation Query – To answer relation queries, KRL projects the KG to the latent space and typically applies graph neural networks (e.g., [41]) as the link prediction operator that aggregates multi-relational graphs to predict the missing relations.

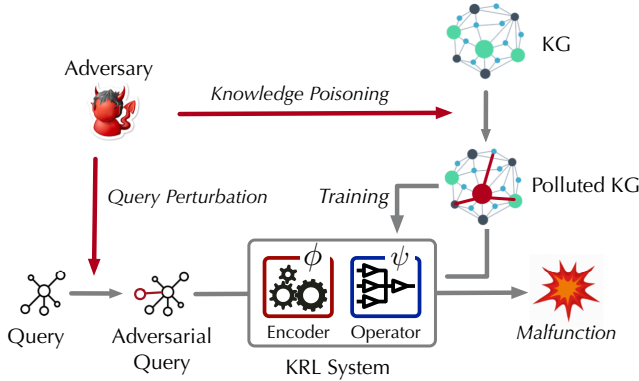


Figure 2: Illustration of ROAR attacks against KRL.

3 Threat Characterization

We systematize the threats to KRL according to the underlying attack vectors and the adversary’s knowledge.

3.1 Adversary model

We first define the adversary model.

Adversary’s objectives – Let Q be the testing query set and Q^* be the set of queries targeted by the adversary ($Q^* \subseteq Q$). In an *untargeted* attack, the adversary aims to force the KRL system to make erroneous reasoning over Q^* ; in a *targeted* attack, the adversary attempts to force the system to return a target answer A when processing Q^* .

In both cases, to be evasive against inspection, the attack must have a limited impact on the system’s performance on non-target queries $Q \setminus Q^*$.

Adversary’s capability – As illustrated in Figure 2, we consider two different attack vectors.

Knowledge Poisoning – Before training, the adversary may commit poisoning facts which are then integrated by KRL to construct the KGs. We argue that this attack vector is practical: most KGs are automatically built using public, crowd-sourced information (e.g., [4]); due to the massive amount of information, it is often challenging to conduct thorough fact checking [48], which opens the door for knowledge poisoning. To make the attack evasive, we require that the number of poisoning facts is limited.

Query Perturbation – At inference, the adversary may also force the KRL system to malfunction by modifying the query by adding misleading variables/relations. To make the attack evasive, we require that (i) only the addition of variables/relations is allowed and (ii) the perturbed query must represent a valid dependency graph with respect to the KG.

Adversary’s knowledge – We consider the adversary’s knowledge regarding the following two components.

Encoder ϕ – The encoder projects KG entities to their embeddings based on their topological and relational structures. With a little abuse of notation, in the following, we use ϕ_v ,

ϕ_G , and ϕ_q to respectively denote the embeddings of entity v , KG G , and query q .

Operator ψ – The relation r -specific operator ψ_r performs geometric transformation to ϕ_v to compute entities with relation r to v . For instance, in Query2Box [38], the KRL consists of two operators, projection and intersection, both implemented as DNNs.

Attack	Adversary’s Capability		Adversary’s Knowledge	
	Knowledge Poisoning	Query Perturbation	Encoder ϕ	Operator ψ
1	✓			
2	✓		✓	
3	✓			✓
4	✓		✓	✓
5		✓		
6		✓	✓	
7		✓		✓
8		✓	✓	✓
9	✓	✓		
10	✓	✓	✓	
11	✓	✓		✓
12	✓	✓	✓	✓

Table 1. A taxonomy of attacks against KRL.

3.2 Attack taxonomy

Based on the adversary’s varying capability and knowledge, we create a taxonomy of 12 attacks against KRL, as summarized in Table 1. Given its unique assumption, each attack tends to require a tailored attack strategy. For instance,

Attack₄ – It uses knowledge poisoning as the attack vector while assuming knowledge about both encoder ϕ and operator ψ . Before training, the adversary crafts poisoning facts to pollute the KG construction in a white-box manner.

Attack₇ – It uses query perturbation as the attack vector and assumes knowledge only about ψ . Without access to ϕ , the adversary may resort to a surrogate encoder $\hat{\phi}$ and generate adversarial queries transferable to the target KRL system at inference time.

Attack₁₀ – It leverages both knowledge poisoning and query perturbation as the attack vectors and assumes knowledge about ϕ but not ψ ; the adversary may thus resort to a surrogate operator $\hat{\psi}$ and optimize the poisoning facts and adversarial queries jointly.

The discussion of the remaining attacks is deferred to §B.

3.3 Challenges

Note that the attacks against KRL bears conceptual similarity to that against conventional classification models (e.g., adversarial evasion [11, 16], model poisoning [21, 42], and backdoor injection [26, 34]). For instance, both KG poisoning and model poisoning use poisoning data to influence the training of target systems, while both query perturbation and adversarial

evasion aim to generate inputs that are perceptually similar to benign ones but cause target systems to malfunction.

However, realizing the attacks against KRL represents a set of unique, non-trivial challenges.

- Projecting KG entities or queries (discrete) to their embeddings (continuous) represents a non-differentiable mapping, making it impractical to directly optimize poisoning facts or adversarial queries, which is especially challenging if the encoder is unknown.

- There exist potentially combinatorial ways to generate poisoning facts with respect to given KGs or adversarial queries with respect to given benign queries, which implies a prohibitive search space.

- In attacks that leverage both poisoning facts and adversarial queries, due to their mutual dependence, every time updating the poisoning facts requires expensive re-computation of the adversarial queries.

In the following, we present ROAR, a new class of attacks against KRL that addresses the above challenges within a novel *Optimization-then-Approximation* (OTA) framework.

4 ROAR Attacks

Next, we give an overview of the OTA framework and then detail the implementation of KG poisoning and query perturbation within this framework. For simplicity, we assume (i) white-box attacks – the adversary has knowledge regarding the KRL system γ (including encoder ϕ and operator ψ); (ii) targeted attacks – the adversary aims to direct the answering of a query set Q^* to the desired answer A (i.e., targeted attacks). We discuss the extension to other settings (e.g., black-box, untargeted attacks) in §4.5.

4.1 Overview of OTA

Recall that KRL traverses across the input spaces (i.e., KG \mathcal{G} and query q), the latent space (i.e., embeddings $\phi_{\mathcal{G}}$ and ϕ_q), and the output space (i.e., answer $\llbracket q \rrbracket$). To mislead KRL to arrive at the target answer A , OTA comprises two key steps:

Optimization – With respect to the desired answer A , OTA optimizes the embeddings, $\phi_{\mathcal{G}}$ in the case of knowledge poisoning and ϕ_q in the case of query perturbation, through back-propagation. Let $\phi_{\mathcal{G}}^+$ and ϕ_q^+ be the updated KG and query.

Approximation – It then projects $\phi_{\mathcal{G}}^+$ (or ϕ_q^+) back to the input space. However, as ϕ is non-differentiable, it leverages attack-specific heuristics to search for KG \mathcal{G}^* (or query q^*) that leads to embeddings to best approximate $\phi_{\mathcal{G}}^+$ (or ϕ_q^+). These two steps are often executed in an interleaving manner until finding proper poisoning facts (or adversarial queries). Below, we elaborate on the implementation of KG poisoning and query perturbation within the OTA framework.

4.2 Knowledge poisoning

Recall that knowledge poisoning aims to direct the answering of Q^* to target answer A by committing poisoning facts \mathcal{F}^* to the construction of KG \mathcal{G} .

Without loss of generality, we define Q^* as queries sharing a common pattern p^* . For instance, p^* can be a specific set of facts forming a logical path (e.g., $p^* = \text{Chrome} \xrightarrow{\text{vulnerable to}} \text{vCVE} \xrightarrow{\text{fixable by}} \text{vmitigation}$). In other words, p^* functions as a *trigger* to invoke KRL to malfunction. Further, to be practical, we assume the number of poisoning facts that can be added is limited by a threshold n_{kp} (i.e., $|\mathcal{F}^*| \leq n_{\text{kp}}$).

Let \mathcal{K}^* collectively denote the anchors entities in p^* (e.g., Chrome in the running example) and the target answer A . To this end, we define \mathcal{F}^* as a set of poisoning facts surrounding \mathcal{K}^* to influence the embeddings of p^* , which in turn misleads the reasoning model to malfunction. This overall flow is illustrated in Figure 3.

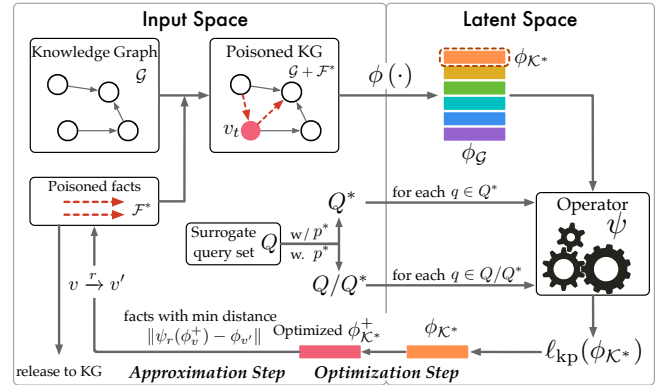


Figure 3: Workflow of knowledge poisoning.

Optimization – At this step, we optimize the embeddings $\phi_{\mathcal{K}^*}$ of \mathcal{K}^* to achieve the attack objective. Note that adding poisoning facts \mathcal{F}^* generally influences not only the embeddings of \mathcal{K}^* but also that of neighboring entities. Yet, due to the locality of \mathcal{F}^* surrounding \mathcal{K}^* and the large scale of \mathcal{G} , we make the assumption that the impact of \mathcal{F}^* on the embeddings of other entities is marginal, which is also confirmed in our empirical evaluation (§5, §6).

The optimization of $\phi_{\mathcal{K}^*}$ carries two objectives: effectiveness – for query $q \in Q^*$, the system returns the desired answer A ; evasiveness – for non-target query $q \in Q \setminus Q^*$, the system returns the ground-truth answer $\llbracket q \rrbracket$. Formally, we define the following loss function: $\ell_{\text{kp}}(\phi_{\mathcal{K}^*})$

$$= \mathbb{E}_{q \in Q^*} \Delta(\gamma(q; \phi_{\mathcal{K}^*}), A) + \lambda \mathbb{E}_{q \in Q \setminus Q^*} \Delta(\gamma(q; \phi_{\mathcal{K}^*}), \llbracket q \rrbracket) \quad (3)$$

where Δ is a metric (e.g., L_2 -norm) to measure the distance between two query answers and λ is the hyper-parameter to balance the two attack objectives. Note that here we assume the embeddings of all the other entities are fixed.

Approximation – At this step, we project the updated embeddings $\phi_{\mathcal{K}^*}^+$ back to the input space to search for the optimal poisoning facts \mathcal{F}^* . Recall that the entity embedding function

ϕ is non-differentiable, it is impractical to directly optimize \mathcal{F}^* . Instead, we adopt a *retrograde search* approach to search for \mathcal{F}^* that leads to embeddings best approximate $\phi_{\mathcal{K}^*}^+$.

Specifically, we use the relation r -specific transformation function ψ_r to assess the quality of candidate facts. Recall that $\psi_r(\phi_v)$ computes entities with relation r to v . We enumerate each candidate fact $v \xrightarrow{r} v'$ wherein $v \in \mathcal{K}^*$ and $v' \in \mathcal{N} \setminus \mathcal{K}^*$ under the updated embedding ϕ_v^+ and select the top- n_{kp} candidate facts with the minimum distance of $\|\psi_r(\phi_v^+) - \phi_{v'}\|$. Intuitively, adding such facts to \mathcal{G} tends to force \mathcal{K}^* to be projected to $\phi_{\mathcal{K}^*}^+$. The algorithm is sketched in Algorithm 1.

Algorithm 1: Retrograde Search

Input: \mathcal{N} – entities in KG \mathcal{G} ; \mathcal{K}^* – anchors of trigger pattern p^* ;
 ϕ_v^+ – updated embedding of $v \in \mathcal{K}^*$; $\phi_{v'}$ – embedding of
 $v' \in \mathcal{N} \setminus \mathcal{K}^*$; ψ_r – relation r -specific embedding function;
 n_{kp} – budget of poisoning facts

Output: \mathcal{F}^* – poisoning facts

```
// initialize
1  $\mathcal{L} \leftarrow \emptyset$ ;
2 foreach  $v \in \mathcal{K}^*$  do
3   foreach  $v' \in \mathcal{N} \setminus \mathcal{K}^*$  do
4     foreach  $r \in \mathcal{R}$  do
5       // compute fitting scores
6       if  $v \xrightarrow{r} v'$  is legitimate then
7         compute  $\|\psi_r(\phi_v^+) - \phi_{v'}\|$ ;
7         add  $\langle v \xrightarrow{r} v', \|\psi_r(\phi_v^+) - \phi_{v'}\| \rangle$  to  $\mathcal{L}$ ;
8 sort  $\mathcal{L}$  in descending order of distance ;
9 return the top- $n_{kp}$  facts in  $\mathcal{L}$  as  $\mathcal{F}^*$ ;
```

The overall complexity of Algorithm 1 is $O(|\mathcal{N}| |\mathcal{K}^*| |\mathcal{R}|)$, where $|\mathcal{N}|$, $|\mathcal{K}^*|$, and \mathcal{R} respectively denote the numbers of entities in \mathcal{G} , anchors in trigger pattern p^* , and relation types. Further, by taking into account the domain constraints of \mathcal{K}^* (e.g., certain facts are implausible), the practical complexity tends to be much lower.

4.3 Query perturbation

Query perturbation attempts to direct the answering of Q^* to target answer A by generating adversarial query q^* from its benign counterpart q . We consider q^* as the conjunction of q and additional logical constraint q^+ : $q^* = q \wedge q^+$. To make the perturbation evasive, we require that (i) the number of logical paths in q^+ is limited by a threshold n_{qp} and (ii) the dependency graph of q^* is valid with respect to \mathcal{G} .

Note that while there are potentially combinatorial ways to generate q^+ , it is often effective to limit q^+ to the vicinity of ground-truth answer $\llbracket q \rrbracket$, which results in more direct influence on altering the query answer.

At a high level, query perturbation adopts the OTA framework. At the optimization step, we optimize the embedding ϕ_{q^*} of q^* with respect to the attack objective; at the approximation step, we further search for potential perturbation q^+ that leads to the embedding most similar to ϕ_{q^*} . Below we elaborate on these two steps.

Optimization – At this step, we optimize the embedding ϕ_{q^*} with respect to target answer A . Recall that q^* is the conjunction of query q and perturbation q^+ . We thus define the following loss function:

$$\ell_{qp}(\phi_{q^+}) = \Delta(\psi_{\wedge}(\phi_q, \phi_{q^+}), A) \quad (4)$$

where ψ_{\wedge} is the relation \wedge -specific transformation function, Δ is the same distance function as in Eq. 3, and ϕ_q is computed using the current embedding model. We then optimize ϕ_{q^+} via backpropagation.

Approximation – At this step, we search for candidate perturbation q^+ (input space) that leads to embeddings best approximating ϕ_{q^+} .

Recall that in the embedding space q^+ is represented as a directed acyclic graph, which starts with the embeddings of its anchor entities, follows the geometric transformation of its relations, and eventually reaches ϕ_{q^+} . We thus reverse this process to reconstruct q^+ . However, the complexity of brute-force search (e.g., breadth-first search) grows exponentially with the search depth. Instead, we adopt *beam search* [43], a greedy strategy, to search for q^+ .

Specifically, starting with the entity closest to ϕ_{q^+} in the latent space as the root, we expand q^+ in a level-wise manner until reaching any pre-defined anchor entities. At each level, the search enumerates all the neighboring entities in \mathcal{G} , constructs the corresponding structures, and selects the top- n_{qp} candidate structures that lead to embeddings closest to ϕ_{q^+} . A running example is illustrated in Figure 4.

The search complexity depends on the depth of q^+ , the perturbation budget n_{qp} , and the number of candidate entities in \mathcal{G} . In the worst case, the expansion at each level examines $|\mathcal{N}|$ candidate structures and selects the top- n_{qp} ones, thus featuring the complexity of $O(n_{qp} |\mathcal{N}|)$. As the depth of q^+ is less than $\varnothing_{\mathcal{G}}$, the diameter of \mathcal{G} , the overall complexity is thus $O(n_{qp} \varnothing_{\mathcal{G}} |\mathcal{N}|)$. In practice, however, as the number of candidate entities is much smaller than $|\mathcal{N}|$, the practical complexity tends to be much lower.

4.4 Knowledge-Query co-optimization

Recall that to direct the answering of a query set Q^* (that shares a specific pattern p^*) to target answer A , the adversary either commits poisoning facts \mathcal{F}^* to \mathcal{G} or perturbs the queries in Q^* . If the adversary is able to leverage both knowledge poisoning and query perturbation, by accounting for the possible perturbation to Q^* (at inference time), it is possible to construct more effective poisoning facts \mathcal{F}^* . We thus propose a co-optimization framework that optimizes poisoning knowledge and adversarial queries jointly, leading to more effective attacks.

As sketched in Algorithm 2, the co-optimization attack iterates between knowledge poisoning and query perturbation: at the i -th iteration, in the knowledge poisoning stage, it generates poisoning facts with respect to the current adversarial

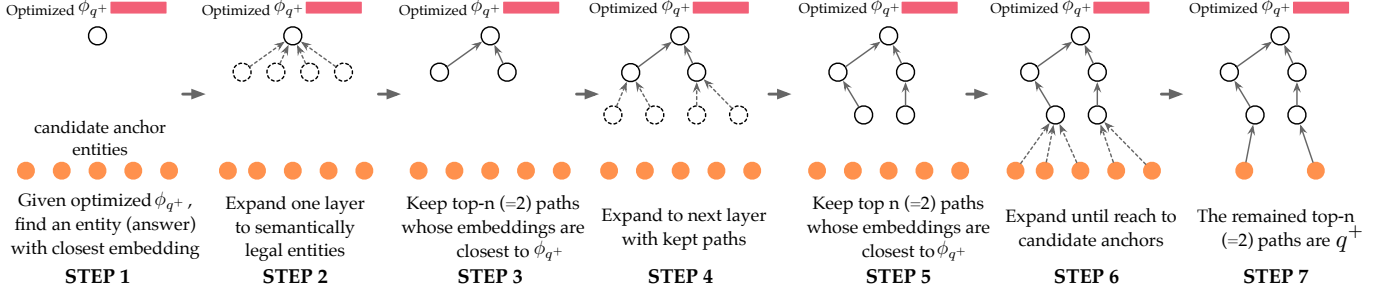


Figure 4: Illustration of constructing q^+ via beam search.

Algorithm 2: Knowledge-Query Co-optimization

Input: Q^* – target query set; \mathcal{G} – KG; n_{iter} – number of iterations
Output: poisoning facts to \mathcal{G} ; adversarial queries of Q^*

```

// initialize
1  $\mathcal{L} \leftarrow \emptyset$ ;
2  $Q^{(0)} \leftarrow Q^*$ ;
3 for  $i = 1, \dots, n_{\text{iter}}$  do
  // knowledge poisoning
4   generate poisoning facts  $\mathcal{F}^*$  with respect to  $Q^{(i-1)}$ ;
5   add  $\mathcal{F}^*$  to  $\mathcal{G}$  as  $\mathcal{G}^{(i)}$ ;
  // query perturbation
6   foreach  $q \in Q^*$  do
7     generate adversarial query  $q^*$  with respect to  $\mathcal{G}^{(i)}$ ;
8     add  $q^*$  to  $Q^{(i)}$ ;
9 return  $\mathcal{G}^{(n_{\text{iter}})} \setminus \mathcal{G}$  and  $Q^{(n_{\text{iter}})}$ ;

```

queries $Q^{(i-1)}$; in the query perturbation, it generates adversarial queries with respect to the updated KG $\mathcal{G}^{(i)}$. The process iterates until convergence.

4.5 Extension

We now discuss the extension of ROAR to other settings.

Black-box attacks – Without knowledge regarding encoder ϕ or operator ψ , the adversary may resort to surrogate models to approximate ϕ or ψ . For instance, it is empirically shown that TransE [9] and TransR [23], two widely used entity embedding models, have fairly similar behavior. It is thus possible to generate poisoning facts/adversarial queries on the surrogate model and then transfer the attack to the target system.

Untargeted attacks – An untargeted attack aims to direct the answering of target queries Q^* to erroneous answers rather than a specific answer A . Thus, at the optimization stage of the attack (Eq. 3 and Eq. 4), instead of minimizing the distance between the answer of $q \in Q^*$ and A , the adversary may maximize the distance between the answer of q and its ground-truth answer $\llbracket q \rrbracket$. For instance, we may re-define Eq. 4 as:

$$\ell_{\text{qp}}(\phi_{q^+}) = -\Delta(\Psi_{\wedge}(\phi_q, \phi_{q^+}), \llbracket q \rrbracket) \quad (5)$$

5 Case Study I: Cyber-Threat Hunting

Next, we conduct an empirical evaluation of ROAR in the concrete case of cyber-threat intelligence reasoning. Our study

is designed to answer the following questions: Q_1 – Is ROAR effective against KRL systems in practice? Q_2 – How does the effectiveness of its variants differ? Q_3 – What factors impact the performance of ROAR?

5.1 Experimental setup

We begin by describing the evaluation setting.

Scenario – With the explosive growth of cyber-threat intelligence, it becomes imperative for security analysts to rely on automated tools to extract useful, actionable intelligence for given incidents [29, 30]. Here, we consider a KRL system built upon cyber-threat KGs (*e.g.*, attack tactics, vulnerabilities, fixes), which supports the following queries:

Vulnerability – Given certain observations regarding the incident (*e.g.*, affected products/versions, attack tactics, or campaigns), it finds the most likely vulnerabilities (*e.g.*, CVEs) that are being exploited.

Mitigation – Beyond the vulnerabilities being attacks, it may further suggest potential solutions (*e.g.*, patches and workarounds) to mitigate such vulnerabilities.

Besides querying for known vulnerabilities, we also consider a zero-day setting wherein the attacks exploit previously unknown vulnerabilities.

CyberKG – We construct the CyberKG using cyber-threat intelligence from three sources: (i) public CVE reports²; (ii) BRON threat graph [20]; (iii) National Vulnerability Database (NVD)³.

– From (i), we collect known CVE as potential vulnerabilities, each associated with *affected product, version, vendor, CWE*⁴, and *threat campaign*.

– From (ii), we extract *attack tactic, technique* and *pattern*, and link them with (i) based on CVE codes.

– From (iii), we collect *mitigation* for each CVE and assign a specific code to each mitigation approach.

The logical structures of the resulted KG is illustrated in Figure 11, with its statistics summarized in Table 14.

Query – To construct queries, for given CVE or *mitigation*, we randomly select anchors from the remaining entities (*e.g.*,

²<https://www.cvedetails.com>

³<https://nvd.nist.gov>

⁴<https://cwe.mitre.org>

affected product, attack pattern, and threat campaign) and formulate the queries based on their logical structures in the KG. Figure 12 shows the logical paths with different anchor entities, which are combined to formulate the query templates as shown in Figure 13. In the evaluation, we generate 500 queries for each query template.

KRL – We apply Query2Box [38], a state-of-the-art KRL approach, to build the reasoning system. Intuitively, by adopting box embeddings (*i.e.*, hyper-rectangles), Query2Box naturally handles first-order conjunctive queries.

Query	MRR	NDCG@5
Vulnerability	0.61	0.76
Mitigation	0.47	0.66

Table 2. KRL performance in cyber-threat hunting.

Metrics – In this case study, we mainly use two metrics to evaluate the performance of KRL and attacks:

MRR – It computes the average reciprocal ranks of all the ground-truth answers across all the queries. This metric measures the global ranking quality of reasoning answers.

NDCG@K – It evaluates the ranking quality of the top- K answers using the NDCG metric [28].

All the measurements range from 0 to 1, with larger values indicating better performance. Table 2 summarizes the performance of the KRL system in cyber-threat hunting.

5.2 Attack implementation

Next, we detail the implementation of ROAR attacks in the case study of cyber-threat hunting.

Attack settings – By default, we set target queries Q^* as that containing a specific pattern $p^* = \text{Android OS} \xrightarrow{\text{vulnerable to}} v_{\text{CVE}} \xrightarrow{\text{fixable by}} v_{\text{mitigation}}$, where Android OS is an anchor entity while both v_{CVE} and $v_{\text{mitigation}}$ are variables. In §5.3, we also consider alternative definitions of p^* .

We consider both targeted and untargeted attacks. In untargeted attacks, the goal is to direct the answering of each query $q \in Q^*$ to an erroneous one (different from its ground-truth $\llbracket q \rrbracket$); in targeted attacks, the goal is to direct the answering of all the queries in Q^* to a target answer A . For vulnerability queries, we set $A = \text{CVE-2021-0471}$, which is a CVE with lower severity among all the Android CVEs; for mitigation queries, we set A as the mitigation of CVE-2021-0471.

Further, it is necessary to ensure the impact of the attacks on benign queries (*i.e.*, without p^*) is limited.

Attack variants – To the best of our knowledge, this is the first work on the security of KRL. We thus mainly compare the performance of different variants of ROAR:

ROAR_{kp}– Relying on knowledge poisoning, the adversary influences KRL by committing poisoning facts to the KG construction, but has no control over the queries. Specifically, ROAR_{kp} commits poisoning facts surrounding Android OS (anchor entity of p^*) and CVE-2021-0471 (target answer A). We

limit the number of poisoning facts by $n_{kp} = 100$.

ROAR_{qp}– Relying on query perturbation, the adversary generates adversarial queries at inference time but has no control over the KG construction. To make the perturbation evasive, we require that (i) the number of logical paths in the perturbation is limited by $n_{qp} = 2$ and (ii) the dependency graph of the perturbed query is valid with respect to the KG.

ROAR_{co}– Leveraging both knowledge poisoning and query perturbation, the adversary optimizes the poisoning facts and adversarial queries jointly.

In all the attacks, we assume the adversary has no control over the training of KRL including (i) how the training set is sampled from the KG and (ii) how the entity embedding and relation transformation models are trained. Thus, all the poisoning facts and/or adversarial queries are crafted on surrogate models.

5.3 Evaluation results

For exposition simplicity, below we highlight the KRL performance variation before and after the attacks. In targeted attacks, “↑” indicates the score increase (*e.g.*, MRR) with respect to target answer A ; in untargeted attacks, “↓” indicates the score decrease with respect to ground-truth answers.

Objective	Query	Attack							
		w/o	ROAR _{kp}	ROAR _{qp}	ROAR _{co}				
Targeted	Vulnerability	.00	.00	.53↑	.57↑	—	—	.99↑	.99↑
	Mitigation	.00	.00	.29↑	.33↑	—	—	.58↑	.60↑
Untargeted	Vulnerability	.56	.75	.34↓	.22↓	.49↓	.48↓	.55↓	.73↓
	Mitigation	.48	.68	.31↓	.20↓	.45↓	.57↓	.48↓	.68↓

Table 3. Overall attack performance in cyber-threat hunting. Note: the values in each cell are MRR (left) and NDCG@5 (right).

Attack effectiveness – Table 3 summarizes the overall attack performance measured by MRR and NDCG@5. Note that without attacks (w/o), none of the queries in Q^* leads to target answer A , due to their irrelevance. We have the following interesting observations.

ROAR_{kp} is more effective in targeted attacks. – ROAR_{qp} seems unable to direct KRL to target answer A . This may be explained by that limited by the perturbation constraints (§4.3), it is difficult to direct the answering of query q to A remotely relevant to $\llbracket q \rrbracket$. In contrast, ROAR_{kp} exerts a more significant influence on KRL by minimizing the distance between the embeddings of pattern p^* (shared by Q^*) and A , leading to more effective targeted attacks.

ROAR_{qp} is more effective in untargeted attacks. – Interestingly, ROAR_{qp} outperforms ROAR_{kp} in untargeted attacks. This may be explained as follows. An untargeted attack succeeds if the answer of query q deviates from $\llbracket q \rrbracket$; the poisoning facts of ROAR_{kp} affects all the queries in the same manner, while in ROAR_{qp}, the perturbation is tailored to each query q , resulting in more effective untargeted attacks.

ROAR_{co} is the most effective attack. – In both targeted and

untargeted cases, ROAR_{co} outperforms the other attacks. For instance, in targeted attacks against vulnerability queries, ROAR_{co} attains 0.99 increase in MRR. This may be attributed to the mutual reinforcement between knowledge poisoning and query perturbation: tailoring poisoning facts to adversarial queries, and vice versa, improves the attack effectiveness.

Objective	Query	Attack			
		ROAR _{kp}		ROAR _{co}	
Targeted	Vulnerability	0.00↓	0.00↓	0.00↓	0.00↓
	Mitigation	0.01↓	0.00↓	0.00↓	0.02↓
Untargeted	Vulnerability	0.00↓	0.02↓	0.00↓	0.00↓
	Mitigation	0.01↓	0.01↓	0.00↓	0.00↓

Table 4. Impact of attacks on non-target queries. Note: the values in each cell are MRR (left) and NDCG@5 (right).

Attack evasiveness – We further measure the impact of the attacks on non-target queries (without pattern p^*). As ROAR_{qp} has no influence on non-target queries, we focus on evaluating ROAR_{kp} and ROAR_{co}, with results shown in Table 4.

ROAR has a limited impact on non-target queries. – Compared with the benign system (cf. Table 2), ROAR_{kp} and ROAR_{co} have negligible influence on the answering of non-target queries. This may be attributed to multiple factors: (i) the limited number of poisoning facts (less than n_{kp}), (ii) the locality of such facts, and (iii) the large size of KG.

Query structures – Recall that the queries are generated following a set of templates (cf. Figure 13). We now evaluate the impact of query structures on the attack performance. We encode the complexity of query q as $n_{\text{path}}-m_{\text{path}}$, where n_{path} is the number of logical paths (from anchors \mathcal{K}_q to answer $\llbracket q \rrbracket$) in q and m_{path} is the length of the longest path. Table 5 breaks down the attack performance according to the setting of n_{path} and m_{path} . We have the following observations.

Attack performance drops with n_{path} . – By increasing the number of logical paths n_{path} but keeping the maximum path length m_{path} fixed, the effectiveness of all the attacks tends to drop. This may be explained as follows. Each logical path in query q represents one constraint on the answer $\llbracket q \rrbracket$; with more constraints, KRL is more robust to local perturbation to either KG or parts of q .

Attack performance improves with m_{path} in targeted cases. – Interestingly, in the targeted cases, the attack performance improves with m_{path} under fixed n_{path} . This may be explained as follows. Longer logical paths in q represent “weaker” constraints, due to the accumulated approximation errors of relation transformation. As p^* is defined as a short logical path, for queries with large m_{path} , p^* tends to dominate the query answering, resulting in more effective attacks.

Surrogate models – Thus far, we assume the surrogate models on which the adversary crafts poisoning facts and/or adversarial queries share the same architectures with the target KRL system. We now examine the scenario wherein the surrogate and actual models differ.

We consider two configurations of the surrogate models

different from the actual models used by KRL (cf. Table 16) in terms of (i) the dimensionality of embeddings and (ii) the depth of DNNs (as relation transformation models), while all the other settings are the same as Table 3. Table 6 shows the attack performance under such alternative surrogate models.

ROAR transfers across different embedding models. – By comparing Table 6 and Table 3, it is observed that while the attack performance drops under the alternative settings, due to the discrepancy between the actual and surrogate models, the decrease is marginal, indicating the transferability of ROAR across different models. This may be explained by that many KG embedding methods demonstrate fairly similar behavior [18]. It is therefore possible to transfer attacks across different embedding models.

KG-Query interaction – We further evaluate the interaction between the attack vectors of knowledge poisoning and query perturbation in ROAR_{co}. Specifically, we evaluate the attack performance as a function of n_{kp} (number of injected poisoning facts) and n_{qp} (number of perturbed logical paths), with results summarized in Figure 5.

There exists an “mutual reinforcement” effect. – In both targeted and untargeted cases, with n_{qp} fixed, slightly increasing n_{kp} significantly improves the attack performance. For instance, in targeted cases, when $n_{kp} = 0$, NDCG@5 remains 0 regardless of the setting of n_{kp} ; if $n_{kp} = 50$, even setting $n_{qp} = 1$ leads to NDCG@5 over 0.5. This indicates that knowledge poisoning greatly boosts the effectiveness of query perturbation and also validates the analysis in §4.4.

The effect is even more evident in untargeted attacks. – It is also observed that ROAR achieves its maximum effectiveness in untargeted attacks with n_{kp} and n_{qp} lower than the case of targeted attacks. This is explained by that without the need to direct KRL to a specific answer A , untargeted attacks are relatively “easier” than targeted attacks, making the mutual reinforcement even more significant.

We also observe similar trends measured by MRR with results shown in Figure 14 (§E).

Alternative p^* pattern – The pattern p^* serves a trigger to invoke KRL to malfunction in ROAR_{kp} and ROAR_{co}. Here, we consider alternative definitions of p^* and evaluate its impact on the attack performance. Specifically, besides its default definition (with Android OS as anchor) in §5.2, we consider two other definitions as listed in Table 7: the one has Port Scanning (which refers to an *attack pattern*) as its anchor and its logical path is of length 2; the other has T1033 (which refers to an *attack technique* of “system owner/user discovery technique”⁵) as its anchor and is of length 3.

p^* with shorter paths leads to more effective attacks. – In Figure 6, we compares the attack performance of ROAR_{kp} and ROAR_{co} under varying definitions of p^* in both targeted and untargeted cases. Observe that the attack effectiveness decreases as the length of p^* grows. This can be explained as

⁵<https://attack.mitre.org/techniques/T1033/>

Objective	Attack	Query Topological Structure ($n_{\text{path}}-m_{\text{path}}$)																	
		3-1		3-2		3-3		5-1		5-2		5-3		7-1		7-2		7-3	
Targeted	w/o	0.00	0.00	0.00	0.00	0.00	0.00	0.00	0.00	0.00	0.00	0.00	0.00	0.00	0.00	0.00	0.00	0.00	
	ROAR _{kp}	0.51↑	0.56↑	0.78↑	0.81↑	0.78↑	0.81↑	0.37↑	0.40↑	0.63↑	0.71↑	0.66↑	0.71↑	0.23↑	0.27↑	0.38↑	0.42↑	0.39↑	0.44↑
	ROAR _{qp}	—	—	—	—	—	—	—	—	—	—	—	—	—	—	—	—	—	—
	ROAR _{co}	0.98↑	0.98↑	1.00↑	1.00↑	1.00↑	1.00↑	0.97↑	0.98↑	1.00↑	0.99↑	1.00↑	1.00↑	0.94↑	0.96↑	1.00↑	1.00↑	1.00↑	1.00↑
Untargeted	w/o	0.59	0.83	0.52	0.75	0.52	0.74	0.60	0.78	0.56	0.75	0.54	0.72	0.60	0.76	0.56	0.72	0.58	0.72
	ROAR _{kp}	0.35↓	0.24↓	0.31↓	0.30↓	0.42↓	0.40↓	0.34↓	0.19↓	0.34↓	0.25↓	0.35↓	0.28↓	0.31↓	0.12↓	0.33↓	0.09↓	0.36↓	0.11↓
	ROAR _{qp}	0.50↓	0.54↓	0.51↓	0.66↓	0.51↓	0.65↓	0.50↓	0.41↓	0.49↓	0.46↓	0.47↓	0.44↓	0.50↓	0.37↓	0.47↓	0.41↓	0.49↓	0.41↓
	ROAR _{co}	0.58↓	0.81↓	0.52↓	0.75↓	0.52↓	0.74↓	0.58↓	0.74↓	0.54↓	0.73↓	0.53↓	0.71↓	0.57↓	0.70↓	0.55↓	0.71↓	0.57↓	0.71↓

Table 5. Topological complexity of queries on the attack performance. Note: the values in each cell are MRR (left) and NDCG@5 (right).

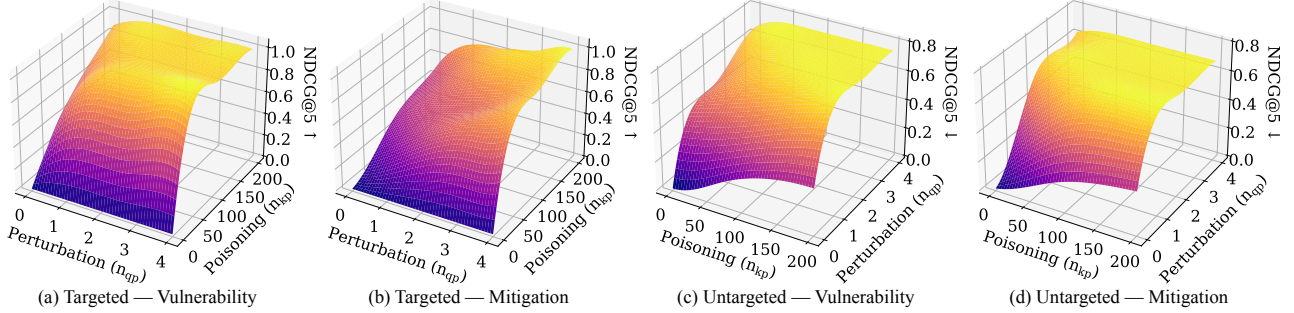


Figure 5: NDCG@5 variation of ROAR_{co} as a function of knowledge poisoning budget (n_{kp}) and query perturbation budget (n_{qp}).

Objective	Query	Attack					
		ROAR _{kp}	ROAR _{qp}	ROAR _{co}			
Embedding Dimensionality = 200, DNN Depth = 1							
Targeted	Vulnerability	.48↑	.55↑	—	—	.96↑	.99↑
	Mitigation	.26↑	.31↑	—	—	.50↑	.55↑
Untargeted	Vulnerability	.34↓	.22↓	.47↓	.44↓	.51↓	.70↓
	Mitigation	.27↓	.21↓	.40↓	.54↓	.44↓	.62↓
Embedding Dimensionality = 500, DNN Depth = 4							
Targeted	Vulnerability	.50↑	.56↑	—	—	.91↑	.95↑
	Mitigation	.27↑	.33↑	—	—	.52↑	.54↑
Untargeted	Vulnerability	.30↓	.19↓	.44↓	.36↓	.49↓	.63↓
	Mitigation	.22↓	.15↓	.37↓	.42↓	.40↓	.61↓

Table 6. Attack performance under alternative surrogate models.

Anchor of p^*	Android OS	Port Scanning	T1033
Category	Product	Attack pattern	Technique
Length (Vulnerability)	1 hop	2 hop	3 hop
Length (Mitigation)	2 hop	3 hop	4 hop

Table 7. Alternative definitions of p^* .

follows. As the poisoning facts are selected surrounding the anchors, their influence tends to fade as the distance between the anchors and the answers. Further, while ROAR_{kp} is inefficient under the setting of p^* starting with T1033, ROAR_{co} is much less sensitive to the setting of p^* (e.g., MRR ≥ 0.39 and NDCG@5 ≥ 0.42), indicating the necessity of co-optimizing poisoning facts and adversarial queries.

Zero-day threats – We further evaluate the performance of ROAR in the scenario of *zero-day* threats, wherein the threats exploit previously unknown vulnerabilities, which often result in consequential damages in practice [8]. We simulate the zero-day case by randomly removing 30% CVEs (from 2020 to 2021) from the KG as the zero-day vulnerabilities, then gen-

erating queries with ground-truth answers among the deleted CVEs. The reasoning task is to search for potential *mitigation* for given incidents. Intuitively, it is possible to find correct mitigation even though the vulnerability is unknown based on similar vulnerabilities (i.e., approximate query). Meanwhile, the attacks aims to mislead KRL to erroneous suggestions (untargeted) or a specific *mitigation A* = MITI-72591⁶ (targeted).

Objective	Attack							
	w/o	ROAR _{kp}	ROAR _{qp}	ROAR _{co}				
Targeted	.00	.00	.34↑	.40↑	—	—	.47↑	.55↑
Untargeted	.39	.61	.20↓	.22↓	.30↓	.44↓	.39↓	.59↓

Table 8. Attack performance against zero-day threat queries.

ROAR is also effective against approximate queries. – Table 8 presents the attack performance in zero-day case. Comparing with Table 3, we have similar observations that (i) ROAR_{kp} is more effective than ROAR_{qp} in targeted attacks; (ii) ROAR_{qp} is more effective than ROAR_{kp} in untargeted attacks; and (iii) ROAR_{co} is the most effective among the three.

Also, note that ROAR is marginally less effective against approximate queries, due to the missing links (i.e., *Vulnerability*) on the paths from anchor entities to answers (*Mitigation*). However, as similar vulnerabilities tend to share mitigation, ROAR is still able to craft effective poisoning facts/adversarial queries to mislead KRL.

6 Case Study II: Drug Repurposing

In the case of cyber-threat hunting, we evaluate ROAR over queries regarding KG entities. Below, we further evaluate

⁶<https://source.android.com/security/bulletin/2021-04-01>

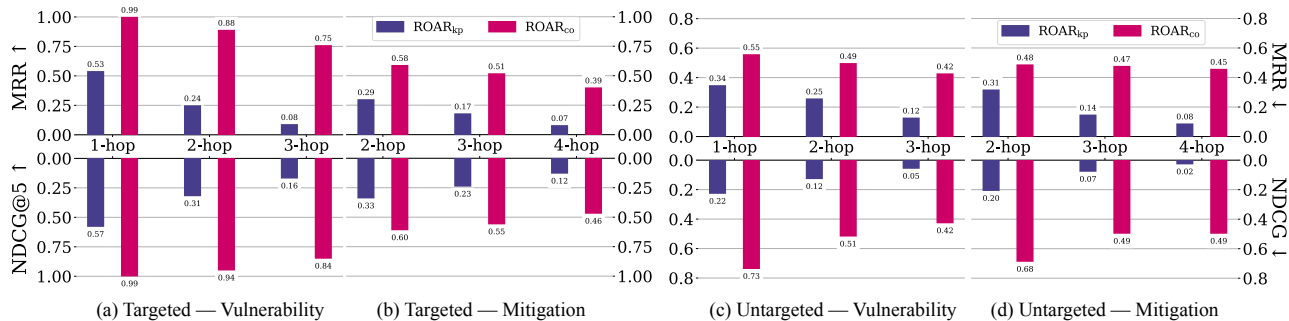


Figure 6: Attack performance under alternative definitions of p^* .

ROAR over queries regarding KG relations in the concrete case of drug repurposing reasoning.

6.1 Experimental setup

We begin by describing the evaluation setting.

Scenario – Drug repurposing aims to find potential therapeutic values or unknown side effects of new drugs [32, 36] by exploring the interactions between drugs, diseases, and human genes. To this end, we consider a KRL system built upon knowledge regarding drugs, diseases, and genes, which supports the following queries:

Drug-disease interaction – Given a drug-disease pair with their relevant properties, it determines the drug’s effect on the disease (*e.g.*, highly/mildly effective).

Drug-gene interactions – Given a drug-gene pair with their relevant properties, it determines the gene’s effect on the drug’s functionality (*e.g.*, suppression/acceleration).

Both types of queries can be formulated as reasoning about the relation $r_\gamma \in \mathcal{R}$ between a given pair of KG entities v, v' : $q[r_\gamma] = r_\gamma. \exists v \xrightarrow{r_\gamma} v'$.

DRKG – We use the Drug Repurposing Knowledge Graph (DRKG) [1] as the underlying KG, which is synthesized from public medical databases. Table 15 lists the stats of DRKG. In particular, there are 10 different drug-disease relations and 34 drug-gene relations.

Queries – To construct the queries, we randomly sample 80K drug-disease and 200K drug-gene pairs and also include their 2-hop neighboring entities as their relevant properties. We use 5% of the queries as the testing set and the remaining as the training set for KRL.

KRL – We instantiate GQE [19] as the encoders and R-GCN [41] as the operators of the KRL system. Intuitively, R-GCN aggregates multi-relational graphs with GCN layers [22], thereby able to aggregate query embeddings to predict missing relations.

Query	HIT@1
Drug-Disease	0.73
Drug-Gene	0.77

Table 9. KRL performance in drug repurposing.

Metrics – As the answer of a relation query is given as the ranking of possible relations, in the evaluation, we mainly use HIT@K ($K = 1$ by default) as the metric: for each query, it checks whether the top-K answers contain the ground-truth answer (*i.e.*, a binary indicator). The results are then averaged across all the queries. Table 9 shows the performance of KRL in this case.

6.2 Attack implementation

Next, we detail the implementation of ROAR in drug repurposing reasoning.

Attack settings – By default, we set target queries Q^* as that contains trigger $p^* = \text{Nervous System} \xrightarrow{\text{includes}} v_{\text{drug}}$, where Nervous System is an Anatomical Therapeutic Chemical (ATC) category as the anchor and v_{drug} is a variable. Intuitively, the adversary aims to influence the reasoning regarding all the drugs in this ATC category.

We consider both targeted and untargeted attacks. In targeted cases, the goal is to direct the answering each query $q \in Q^*$ to a specific relation $A = \text{biomarker-of}$; in untargeted cases, the goal is to deviate the answering of q from its ground-truth answer $\llbracket q \rrbracket$.

Attack variants – We compare the performance of different variants of ROAR.

ROAR_{kp}– It influences KRL by injecting poisoning facts to the KG. Given that genes and diseases are public, verifiable knowledge, it is more evasive to inject poisoning facts surrounding drugs. Thus, ROAR_{kp} attaches poisoning facts to Nervous System (p^* ’s anchor).

ROAR_{qp}– It directly attaches additional logical paths (from the KG) to the drug entity of the query. As all the related properties of a drug are within 2 hops, ROAR_{qp} also searches for logical paths within 2 hops of the drug.

ROAR_{co}– Leveraging both knowledge poisoning and query perturbation, ROAR_{co} optimizes the poisoning facts and adversarial queries jointly.

Given that DRKG (average density 120.8) is much denser than CyberKG (average density 8.7), we limit the number of injected poisoning facts by $n_{kp} = 400$ and the number of perturbed logical paths $n_{qp} = 20$ by default. The setting of other parameters is deferred to Table 16.

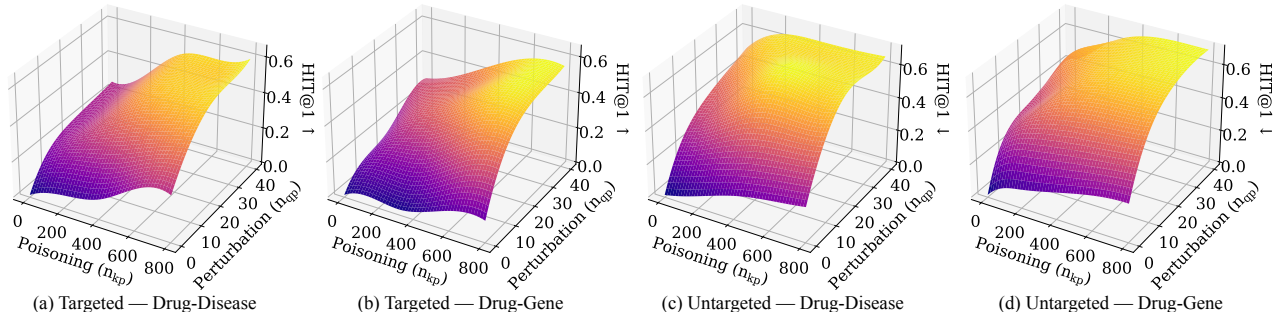


Figure 7: HIT@1 variation of $ROAR_{co}$ when adjusting KG poisoning budget (n_{kp}) and query perturbation budget (n_{qp})

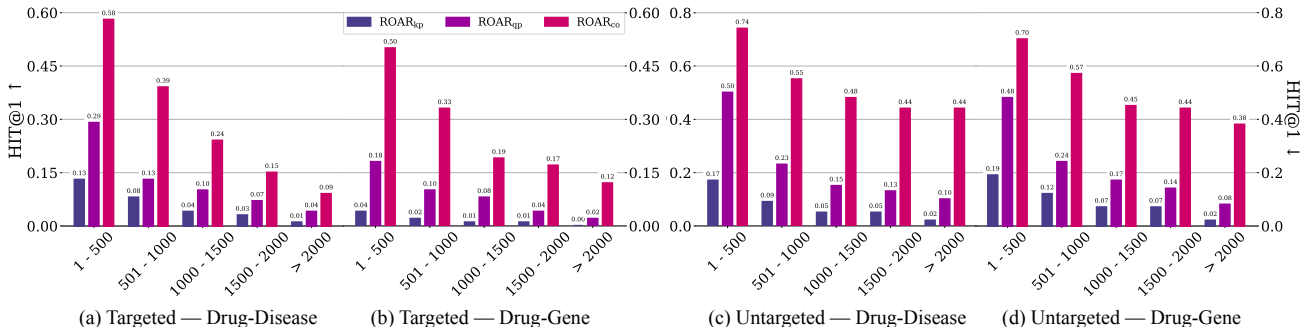


Figure 8: Attack performance with respect to the number of properties associated with drug entities.

6.3 Evaluation results

The evaluation below focuses on three aspects: (i) the overall attack effectiveness and evasiveness (ii) the interaction between the two attack vectors, and (iii) the impact of different factors on the attack performance.

Objective	Query	Target Q^*				Non-Target $Q \setminus Q^*$	
		w/o	$ROAR_{kp}$	$ROAR_{qp}$	$ROAR_{co}$	$ROAR_{kp}$	$ROAR_{co}$
Targeted	Drug-Disease	.00	.10 \uparrow	.22 \uparrow	.46 \uparrow	.03 \downarrow	.03 \downarrow
	Drug-Gene	.04	.03 \uparrow	.14 \uparrow	.40 \uparrow	.01 \downarrow	.00 \downarrow
Untargeted	Drug-Disease	.68	.13 \downarrow	.38 \downarrow	.65 \downarrow	.02 \downarrow	.03 \downarrow
	Drug-Gene	.74	.15 \downarrow	.37 \downarrow	.62 \downarrow	.03 \downarrow	.01 \downarrow

Table 10. Overall attack performance of ROAR in drug repurposing.

Attack effectiveness – Table 10 presents the overall performance of ROAR measured by HIT@1. Similar to the case of cyber-threat hunting, observe that $ROAR_{co}$ outperforms the other variants in both targeted and untargeted cases, due to the interactions between knowledge poisoning and query perturbation. Besides, we have the following observation:

$ROAR_{qp}$ is more effective than $ROAR_{kp}$. – Across all the settings, $ROAR_{qp}$ consistently outperforms $ROAR_{kp}$. This may be explained as follows: $ROAR_{kp}$ influences the drug-disease (or drug-gene) relation by attaching poisoning facts to the ATC entity, which in turn influences the drug entity; meanwhile, $ROAR_{kp}$ directly attaches perturbation to the drug entity, leading to more effective attacks.

Attack evasiveness – Table 10 also shows the impact of ROAR on non-target queries $Q \setminus Q^*$. Observe that the HIT@1 score drops no more than 0.03 across all the settings, indicating the fairly marginal impact of ROAR.

KG-Query interaction – We further evaluate the interaction between knowledge poisoning and query perturbation in the case of drug repurposing. We evaluate the attack performance as a function of n_{kp} and n_{qp} , with results summarized in Figure 7.

Similar to §5, we have the observations below. (i) There exists an “mutual reinforcement” effect between the two attack vectors. The injected poisoning facts greatly boots the effectiveness of adversarial queries in directing the answering of relation queries. (ii) This reinforcement effect seems more evident in untargeted attacks, given that an untargeted attack succeeds if the drug-disease (or drug-gene) relations are mispredicted while a targeted attack requires the relation to be predicted to target answer A.

Objective	Query	#Dim = 100, #Layer = 1			#Dim = 400, #Layer = 4		
		$ROAR_{kp}$	$ROAR_{qp}$	$ROAR_{co}$	$ROAR_{kp}$	$ROAR_{qp}$	$ROAR_{co}$
Targeted	Drug-Disease	.10 \uparrow	.18 \uparrow	.41 \uparrow	.05 \uparrow	.12 \uparrow	.33 \uparrow
	Drug-Gene	.01 \uparrow	.09 \uparrow	.34 \uparrow	.00 \uparrow	.12 \downarrow	.30 \downarrow
Untargeted	Drug-Disease	.11 \downarrow	.35 \downarrow	.62 \downarrow	.10 \downarrow	.24 \downarrow	.51 \downarrow
	Drug-Gene	.15 \downarrow	.33 \downarrow	.57 \downarrow	.06 \downarrow	.28 \downarrow	.49 \downarrow

Table 11. Attack performance under alternative surrogate models in drug repurposing.

Surrogate models – We now evaluate ROAR in the case wherein the surrogate and actual models differ. We consider two configurations of the surrogate models different from the actual models used by KRL (c.f. Table 16) in terms of (i) the embedding dimensionality and (ii) the depth of R-GCN, while all the other settings are the same as Table 10.

It is shown in Table 11 that while the attack performance slightly decreases as the surrogate and actual models differ,

the drop is marginal, especially when the surrogate model is simpler than the actual model (embedding dimensionality = 100, depth of R-GCN = 1), indicating the transferability of ROAR from simpler models to more complicated ones.

Number of properties – Recall that a relation query is a subgraph centering around a drug-disease (or drug-gene) pair, while the surrounding entities represent their descriptive properties. For instance, the neighboring entities of a drug entity describe its biomedical properties (*e.g.*, *ATC* and *side effect*). Figure 8 breaks down the attack performance according to the number of properties associated with drug entities.

Relations with fewer properties are more vulnerable. – It is observed that in both targeted and untargeted cases, the attack performance degrades with the number of properties. This can be explained as follows. For given query q , each property represents one logical constraint on its ground-truth answer $\llbracket q \rrbracket$; more properties make KRL more robust against poisoning facts or adversarial perturbation. Yet, even with more than 2,000 properties, ROAR_{co} still attains high HIT@1 scores, especially in the untargeted cases, indicating the necessity of optimizing poisoning facts and adversarial queries jointly.

7 Discussion

We now explore potential countermeasures against ROAR.

7.1 Potential Countermeasures

Due to the unique characteristics of KRL, the existing defenses against malicious attacks in classification tasks [27, 44, 45] are inapplicable. Thus, we investigate two potential countermeasures tailored to knowledge poisoning and query perturbation, respectively, and further explore their synergy.

Filtering poisoning facts – As poisoning facts are forcefully injected into the KG, they may misalign with their neighboring entities/relations. It is therefore possible to detect and purge them as noisy facts before using the KG in KRL.

To this end, for each fact $v \xrightarrow{r} v'$ in the KG, we apply encoder ϕ and relation r -specific operator ψ_r to assess its “fitness” to the KG. Specifically, we compute the anomaly score of $v \xrightarrow{r} v'$ as: $\|\psi_r(\phi_v) - \phi_{v'}\|$. A higher anomaly score indicates less fitness of $v \xrightarrow{r} v'$. We may remove facts with the highest scores, thereby mitigating the influence of poisoning facts.

In practice, we may first train KRL (including both ϕ and ψ) with the complete KG, prune $m\%$ of the facts with the highest anomaly scores, and then re-train KRL.

Results and analysis – Figure 9 shows the KRL performance on non-target queries and the attack performance on target queries in (a) cyber-threat hunting and (b) drug repurposing. It is observed that as m grows from 0 to 10, in (a) the KRL performance slightly decreases while in (b) the KRL performance slightly improves. We attribute this phenomenon to

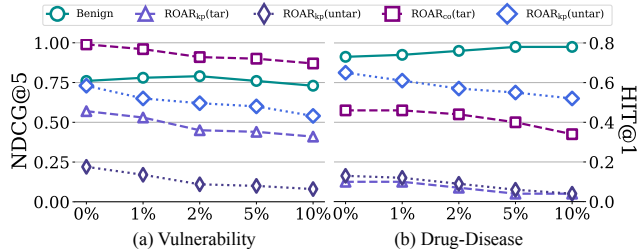


Figure 9: KRL performance on non-target queries and attack performance on target queries. (a) Vulnerability query in cyber-threat hunting; (b) Drug-disease query in drug repurposing.

the density difference of these two KGs (8.7 versus 120.8). For a sparser KG like CyberKG, over-pruning has a negative impact on the KRL performance. In both cases, the attack performance slightly drops with m .

Thus, (i) filtering of poisoning facts may not be suitable for sparse KGs; and (ii) even with a large pruning rate (*e.g.*, 10%), the improvement of attack resilience seems marginal.

Training with adversarial queries – We further consider an adversarial training [27] strategy to defend against query perturbation. Intuitively, during KRL training, we generate an adversarial version q^* for each query q using ROAR_{qp} and add $(q^*, \llbracket q \rrbracket)$ to the training set, where $\llbracket q \rrbracket$ is q ’s ground-truth answer. Note that here we use the untargeted ROAR_{qp} (Eq. 5) to generate q^* .

Results and analysis – Similar to ROAR_{qp}, robust training has a threshold n_{qp}^d that limits the number of perturbed paths. We measure the performance of ROAR_{co} under varying settings of n_{qp} and n_{qp}^d , with results shown in Figure 10.

Observe that across all the cases, robust training greatly reduces the attack performance, especially against untargeted attacks when $n_{qp}^d \geq n_{qp}$. However, robust training also significantly impacts the KRL performance, resulting in over 0.19 NDCG@5 drop in cyber-threat hunting and over 0.11 HIT@1 drop in drug repurposing. Further, it is inherently ineffective against ROAR_{kp}, which does not rely on adversarial queries.

Synergy – Finally, we integrate the two defenses above and explore their synergy. We set pruning rate $m = 1\%$ and $n_{qp}^d = 2/20$ for cyber-threat hunting/drug repurposing. The attacks follow the default setting in Table 16.

Query	Objective	Target Q^*			Non-Target $Q \setminus Q^*$
		ROAR _{kp}	ROAR _{qp}	ROAR _{co}	
Vulnerability	Targeted	0.05↓	—	0.26↓	0.02↓
	Untargeted	0.08↓	0.20↓	0.36↓	
Drug-Disease	Targeted	0.02↓	0.12↓	0.15↓	0.04↑
	Untargeted	0.06↓	0.18↓	0.30↓	

Table 12. Attack performance and KRL performance against the integrated defense.

Results and analysis – The results are shown in Table 12. Comparing with the original attack performance (*cf.* Table 3 and 10), the integrated defense reduces the attack effectiveness by a large margin, even though it does not completely block ROAR; moreover, it alleviates the negative impact on the KRL

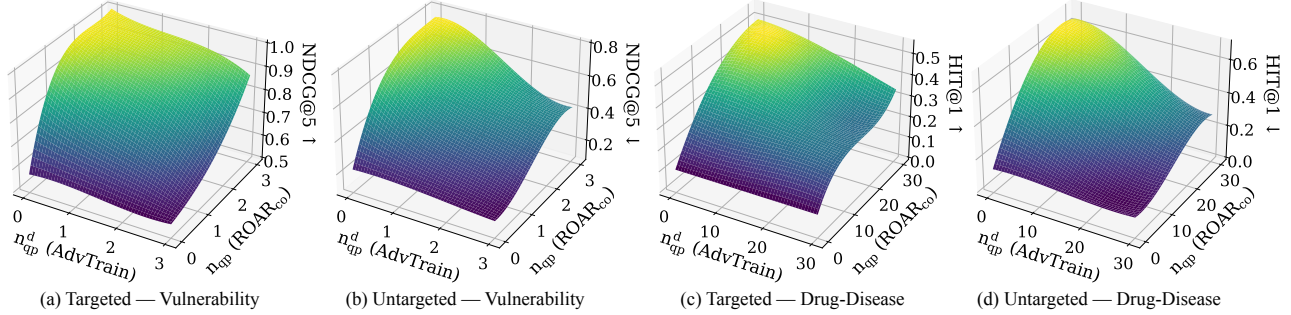


Figure 10: Performance of ROAR_{co} against robust training with respect to varying settings of n_{qp} and n_{qp}^d .

performance and even improves the HIT@1 score in drug repurposing! Thus, the integration of multiple defenses seems a promising direction worth further investigation.

7.2 Limitations

We now discuss the limitations of this work.

Alternative reasoning tasks – We mainly focus on reasoning tasks with one target answer (entity/relation), while there exist other reasoning tasks (*e.g.*, path reasoning [46] aims to find a path with given starting and end entities). Intuitively, ROAR is ineffective in such tasks as it requires knowledge about the logical path and then perturbs intermediate entities on the path. We consider exploring the vulnerability of alternative reasoning tasks as our ongoing research.

Input-space attacks – While ROAR directly operates on KGs (or queries) in the logical space, there are scenarios in which KGs (or queries) are extracted from real-world inputs. For instance, cyber-threat queries may be generated by software testing and inspection. In such scenarios, it requires the perturbation to KGs (or queries) to be mapped to valid real-world inputs (*e.g.*, software). While input-space attacks are an ongoing area of research [35], we consider realizing ROAR in the input space represents unique challenges.

Integration of defenses – While it is shown that integrating filtering poisoning knowledge and training with adversarial queries greatly improves the attack resilience, it is unclear how to optimally integrate such defenses to balance the factors of attack robustness (*e.g.*, against adaptive attacks), impact on KRL performance, and training cost. We consider answering these questions critical for improving the robustness of KRL in a practical setting.

8 Related Work

Next, we survey the literature relevant to this work.

Knowledge representation learning – Knowledge graphs (KGs) represent valuable information sources in various domains [30, 50]. Recent years have witnessed significant progress in using machine learning to reason over KGs. The existing work can be roughly classified into two categories.

One line of work aims to develop effective KG embeddings [10, 24, 31, 47, 49] such that the semantics of KG entities/relations are effectively captured by their latent representations for applications such as link prediction [13, 14]. Another line of work focuses on directly making predictions about complex logical queries [19, 37–39] such as first-order conjunctive queries. The KRL models considered in this paper belong to this category.

Machine learning security – With their increasing use in security-sensitive domains, machine learning (ML) models are becoming the targets for malicious attacks [7]. A variety of attack vectors have been exploited: adversarial evasion crafts adversarial inputs to force the target model to malfunction [11, 16]; model poisoning modifies the target model’s behavior (*e.g.*, performance drop) via polluting its training data [21]; backdoor injection creates a trojan model such that any trigger-embedded input is likely to be misclassified [26]; and functionality stealing constructs a replicate model functionally similar to a victim model [33].

In response, another line of work strives to improve the resilience of ML models against such attacks. For instance, against adversarial evasion, existing defenses explore new training strategies (*e.g.*, adversarial training) [27] and detection mechanisms [15]. Yet, such defenses often fail when facing even stronger attacks [6, 25], resulting in a constant arms race between the attackers and defenders.

Despite the intensive research on KRL and ML security in parallel, the security of KRL is largely unexplored. This work represents an initial step to bridge this gap.

9 Conclusion

This work represents an in-depth study on the security of knowledge representation learning (KRL). We present ROAR, a new class of attacks that instantiate a variety of threats to KRL. We demonstrate the practicality of ROAR in two representative security-sensitive applications, raising concerns about the current practice of training and using KRL. Moreover, we discuss potential mitigation, which might shed light on applying KRL in a more secure manner.

References

- [1] DRKG - Drug Repurposing Knowledge Graph for Covid-19. <https://github.com/gnn4dr/DRKG/>.
- [2] Google Knowledge Graph. <https://developers.google.com/knowledge-graph/>.
- [3] Microsoft Academic Knowledge Graph. <https://makg.org/>.
- [4] Wikidata. <https://www.wikidata.org/>.
- [5] YAGO: A High-Quality Knowledge Base. <https://yago-knowledge.org/>.
- [6] Anish Athalye, Nicholas Carlini, and David Wagner. Obfuscated Gradients Give a False Sense of Security: Circumventing Defenses to Adversarial Examples. In *Proceedings of IEEE Conference on Machine Learning (ICML)*, 2018.
- [7] Battista Biggio and Fabio Roli. Wild Patterns: Ten Years after The Rise of Adversarial Machine Learning. *Pattern Recognition*, 84:317–331, 2018.
- [8] Leyla Bilge and Tudor Dumitras. Before We Knew It: An Empirical Study of Zero-Day Attacks in the Real World. In *Proceedings of ACM Conference on Computer and Communications (CCS)*, 2012.
- [9] Antoine Bordes, Nicolas Usunier, Alberto Garcia-Durán, Jason Weston, and Oksana Yakhnenko. Translating Embeddings for Modeling Multi-Relational Data. In *Proceedings of Advances in Neural Information Processing Systems (NeurIPS)*, 2013.
- [10] Antoine Bordes, Nicolas Usunier, Alberto Garcia-Duran, Jason Weston, and Oksana Yakhnenko. Translating Embeddings for Modeling Multi-relational Data. *Advances in neural information processing systems*, 26, 2013.
- [11] Nicholas Carlini and David A. Wagner. Towards Evaluating the Robustness of Neural Networks. In *Proceedings of IEEE Symposium on Security and Privacy (S&P)*, 2017.
- [12] Nilesh Dalvi and Dan Suciu. Efficient Query Evaluation on Probabilistic Databases. *The VLDB Journal*, 16:523–544, 2007.
- [13] Rajarshi Das, Shehzaad Dhuliawala, Manzil Zaheer, Luke Vilnis, Ishan Durugkar, Akshay Krishnamurthy, Alex Smola, and Andrew McCallum. Go for a Walk and Arrive at the Answer: Reasoning Over Paths in Knowledge Bases using Reinforcement Learning. In *Proceedings of International Conference on Learning Representations (ICLR)*, 2018.
- [14] Rajarshi Das, Arvind Neelakantan, David Belanger, and Andrew McCallum. Chains of Reasoning over Entities, Relations, and Text using Recurrent Neural Networks. In *Proceedings of European Chapter of the Association for Computational Linguistics (EACL)*, 2017.
- [15] Timon Gehr, Matthew Mirman, Dana Drachler-Cohen, Petar Tsankov, Swarat Chaudhuri, and Martin Vechev. AI2: Safety and Robustness Certification of Neural Networks with Abstract Interpretation. In *Proceedings of IEEE Symposium on Security and Privacy (S&P)*, 2018.
- [16] Ian Goodfellow, Jonathon Shlens, and Christian Szegedy. Explaining and Harnessing Adversarial Examples. In *Proceedings of International Conference on Learning Representations (ICLR)*, 2015.
- [17] Kelvin Guu, John Miller, and Percy Liang. Traversing Knowledge Graphs in Vector Space. In *Proceedings of Conference on Empirical Methods in Natural Language Processing (EMNLP)*, 2015.
- [18] Kelvin Guu, John Miller, and Percy Liang. Traversing Knowledge Graphs in Vector Space. In *Proceedings of Conference on Empirical Methods in Natural Language Processing (EMNLP)*, 2015.
- [19] William L. Hamilton, Payal Bajaj, Marinka Zitnik, Dan Jurafsky, and Jure Leskovec. Embedding Logical Queries on Knowledge Graphs. In *Proceedings of Advances in Neural Information Processing Systems (NeurIPS)*, 2018.
- [20] Erik Hemberg, Jonathan Kelly, Michal Shlapentokh-Rothman, Bryn Reinstadler, Katherine Xu, Nick Rutar, and Una-May O’Reilly. Linking Threat Tactics, Techniques, and Patterns with Defensive Weaknesses, Vulnerabilities and Affected Platform Configurations for Cyber Hunting. *ArXiv e-prints*, 2020.
- [21] Yujie Ji, Xinyang Zhang, Shouling Ji, Xiapu Luo, and Ting Wang. Model-Reuse Attacks on Deep Learning Systems. In *Proceedings of ACM Conference on Computer and Communications (CCS)*, 2018.
- [22] Thomas N Kipf and Max Welling. Semi-Supervised Classification with Graph Convolutional Networks. *ArXiv e-prints*, 2016.
- [23] Yankai Lin, Zhiyuan Liu, Maosong Sun, Yang Liu, and Xuan Zhu. Learning Entity and Relation Embeddings for Knowledge Graph Completion. In *Proceedings of AAAI Conference on Artificial Intelligence (AAAI)*, 2015.
- [24] Yankai Lin, Zhiyuan Liu, Maosong Sun, Yang Liu, and Xuan Zhu. Learning entity and relation embeddings for knowledge graph completion. In *Proceedings of AAAI Conference on Artificial Intelligence (AAAI)*, 2015.

- [25] Xiang Ling, Shouling Ji, Jiayu Zou, Jiannan Wang, Chunming Wu, Bo Li, and Ting Wang. DEEPSEC: A Uniform Platform for Security Analysis of Deep Learning Model. In *Proceedings of IEEE Symposium on Security and Privacy (S&P)*, 2019.
- [26] Yingqi Liu, Shiqing Ma, Yousra Aafer, Wen-Chuan Lee, Juan Zhai, Weihang Wang, and Xiangyu Zhang. Trojaning Attack on Neural Networks. In *Proceedings of Network and Distributed System Security Symposium (NDSS)*, 2018.
- [27] Aleksander Madry, Aleksandar Makelov, Ludwig Schmidt, Dimitris Tsipras, and Adrian Vladu. Towards Deep Learning Models Resistant to Adversarial Attacks. In *Proceedings of International Conference on Learning Representations (ICLR)*, 2018.
- [28] Frank McSherry and Marc Najork. Computing Information Retrieval Performance Measures Efficiently in the Presence of Tied Scores. In *Proceedings of European Conference on Information Retrieval (ECIR)*, 2008.
- [29] Sudip Mittal, Prajit Kumar Das, Varish Mulwad, Anupam Joshi, and Tim Finin. Cybertwitter: Using Twitter to Generate Alerts for Cybersecurity Threats and Vulnerabilities. In *Proceedings of IEEE/ACM International Conference on Advances in Social Networks Analysis and Mining (ASONAM)*, 2016.
- [30] Sudip Mittal, Anupam Joshi, and Tim Finin. Cyber-all-intel: An AI for Security Related Threat Intelligence. *ArXiv e-prints*, 2019.
- [31] Maximilian Nickel, Lorenzo Rosasco, and Tomaso Poggio. Holographic Embeddings of Knowledge Graphs. In *Proceedings of AAAI Conference on Artificial Intelligence (AAAI)*, 2016.
- [32] Tudor I Oprea, Julie E Bauman, Cristian G Bologa, Tione Buranda, Alexandre Chigaev, Bruce S Edwards, Jonathan W Jarvik, Hattie D Gresham, Mark K Haynes, Brian Hjelle, et al. Drug Repurposing from an Academic Perspective. *Drug Discovery Today: Therapeutic Strategies*, (3-4):61–69, 2011.
- [33] Tribhuvanesh Orekondy, Bernt Schiele, and Mario Fritz. Knockoff Nets: Stealing Functionality of Black-Box Models. In *Proceedings of IEEE Conference on Computer Vision and Pattern Recognition (CVPR)*, 2018.
- [34] Ren Pang, Hua Shen, Xinyang Zhang, Shouling Ji, Yevgeniy Vorobeychik, Xiapu Luo, Alex Liu, and Ting Wang. A Tale of Evil Twins: Adversarial Inputs versus Poisoned Models. In *Proceedings of ACM Conference on Computer and Communications (CCS)*, 2020.
- [35] Fabio Pierazzi, Feargus Pendlebury, Jacopo Cortellazzi, and Lorenzo Cavallaro. Intriguing Properties of Adversarial ML Attacks in the Problem Space. In *Proceedings of IEEE Symposium on Security and Privacy (S&P)*, 2019.
- [36] Sudeep Pushpakom, Francesco Iorio, Patrick A Eyers, K Jane Escott, Shirley Hopper, Andrew Wells, Andrew Doig, Tim Williams, Joanna Latimer, Christine McNamee, et al. Drug Repurposing: Progress, Challenges and Recommendations. *Nature reviews Drug discovery*, 18:41–58, 2019.
- [37] Hongyu Ren, Hanjun Dai, Bo Dai, Xinyun Chen, Michihiro Yasunaga, Haitian Sun, Dale Schuurmans, Jure Leskovec, and Denny Zhou. LEGO: Latent Execution-Guided Reasoning for Multi-Hop Question Answering on Knowledge Graphs. In *Proceedings of IEEE Conference on Machine Learning (ICML)*, 2021.
- [38] Hongyu Ren, Weihua Hu, and Jure Leskovec. Query2box: Reasoning over Knowledge Graphs in Vector Space using Box Embeddings. In *Proceedings of International Conference on Learning Representations (ICLR)*, 2020.
- [39] Hongyu Ren and Jure Leskovec. Beta Embeddings for Multi-Hop Logical Reasoning in Knowledge Graphs. In *Proceedings of Advances in Neural Information Processing Systems (NeurIPS)*, 2020.
- [40] Nir Rosenfeld, Sophie Hilgard, Sai Srivatsa Ravindranath, and David C. Parkes. From Predictions to Decisions: Using Lookahead Regularization. In *Proceedings of Advances in Neural Information Processing Systems (NeurIPS)*, 2020.
- [41] Michael Schlichtkrull, Thomas N Kipf, Peter Bloem, Rianne Van Den Berg, Ivan Titov, and Max Welling. Modeling Relational Data with Graph Convolutional Networks. In *Proceedings of European Semantic Web Conference*, 2018.
- [42] Octavian Suci, Radu Mărginean, Yiğitcan Kaya, Hal Daumé, III, and Tudor Dumitraş. When Does Machine Learning FAIL? Generalized Transferability for Evasion and Poisoning Attacks. In *Proceedings of USENIX Security Symposium (SEC)*, 2018.
- [43] Christoph Tillmann and Hermann Ney. Word Reordering and A Dynamic Programming Beam Search Algorithm for Statistical Machine Translation. *Computational Linguistics*, 29:97–133, 2003.
- [44] Brandon Tran, Jerry Li, and Aleksander Madry. Spectral Signatures in Backdoor Attacks. In *Proceedings of Advances in Neural Information Processing Systems (NeurIPS)*, 2018.

- [45] B. Wang, Y. Yao, S. Shan, H. Li, B. Viswanath, H. Zheng, and B. Y. Zhao. Neural Cleanse: Identifying and Mitigating Backdoor Attacks in Neural Networks. In *Proceedings of IEEE Symposium on Security and Privacy (S&P)*, 2019.
- [46] Xiang Wang, Dingxian Wang, Canran Xu, Xiangnan He, Yixin Cao, and Tat-Seng Chua. Explainable Reasoning over Knowledge Graphs for Recommendation. In *Proceedings of AAAI Conference on Artificial Intelligence (AAAI)*, 2019.
- [47] Zhen Wang, Jianwen Zhang, Jianlin Feng, and Zheng Chen. Knowledge Graph Embedding by Translating on Hyperplanes. In *Proceedings of AAAI Conference on Artificial Intelligence (AAAI)*, 2014.
- [48] Yexiang Xue, Yang Yuan, Zhitian Xu, and Ashish Sabharwal. Expanding Holographic Embeddings for Knowledge Completion. In *Proceedings of Advances in Neural Information Processing Systems (NeurIPS)*, 2018.
- [49] Bishan Yang, Wen-tau Yih, Xiaodong He, Jianfeng Gao, and Li Deng. Embedding Entities and Relations for Learning and Inference in Knowledge Bases. *ArXiv e-prints*, 2014.
- [50] Yongjun Zhu, Chao Che, Bo Jin, Ningrui Zhang, Chang Su, and Fei Wang. Knowledge-driven Drug Repurposing Using a Comprehensive Drug Knowledge Graph. *Health Informatics Journal*, 26:2737–2750, 2020.

A Notations

Table 13 summarizes the important notations.

B Attack Taxonomy

Attack₁, Attack₂, Attack₃ – They use knowledge poisoning as the attack vector but with different knowledge of the encoder ϕ and the operator ψ . The adversary without knowledge of encoder ϕ builds a surrogate one with self-determined embedding dimensionality (Attack₁, Attack₃). The adversary without knowledge of operator ψ crafts an independent model that may function differently (Attack₁, Attack₂).

Attack₅, Attack₆, Attack₈ – They take query perturbation as the attack vector. If the adversary has no knowledge of the reasoning system (Attack₅) or has partial knowledge (Attack₆), it must leverage a surrogate system or partial component for inference-time perturbation. With white-box access (Attack₈), the adversary can directly query the actual system and craft perturbations.

Attack₉, Attack₁₁, Attack₁₂ – They operate on both KG and queries as attack vectors. The major difference is leveraging an entire surrogate system (Attack₈), or a surrogate encoder ϕ

Notation	Definition
Data – knowledge graph related	
\mathcal{G}	a knowledge graph
$\langle v, r, v' \rangle$	a KG fact from entity v to v' with relation r
$\mathcal{N}, \mathcal{E}, \mathcal{R}$	entity, edge, and relation set of \mathcal{G}
\mathcal{F}	all facts in KG
\mathcal{F}^*	a fact set contributed by the attacker
Data – query related	
q, Q	a single query; a query set
$\llbracket q \rrbracket$	q 's ground-truth answer(s)
A	the targeted answer
p^*	the targeted logical path for attack
\mathcal{K}_q	anchor entities of query q
\mathcal{K}^*	anchor entities of p^*
Q^*	a query set that each included query has p^*
$Q \setminus Q^*$	a query set that each included query doesn't have p^*
q^+	the generated perturbations on q
q^*	conjunction of q and q^+ , i.e., the perturbed query
Model or embedding related	
γ	the reasoning system
ϕ	the encoder for generating entity embeddings
Ψ, Ψ_r	the (relation r -specific) operator
$\phi_{\mathcal{G}}$	embeddings of all KG entities
ϕ_v	entity v 's embedding
ϕ_q	q 's embedding
Other parameters	
n_{kp}	KG poisoning budget
n_{qp}	query perturbation budget
n_{qp}^d	query perturbation budget used by the defender
n_{iter}	Number of iterations in co-optimization

Table 13. Notations, definitions, and categories.

with the actual reasoning operator Ψ (Attack₁₁), or white-box access to both ϕ and Ψ (Attack₁₂) and manipulate poisoning facts with query perturbations.

C KG Statistics

Here, we present the statistics of KGs used in §5 and §6.

CyberKG – Table 14 lists statistics of entities/relations of our cyber-domain KG, whose structure is shown in Figure 11. We add the reverse facts to augment KG during evaluations.

Query templates follow Figure 13. The first 3 rows (path number=2/3/5) are used as training-query structures, while the last 3 rows (path number = 3/5/7) are used for evaluation. We follow Figure 12 to sample each query path from KG with a fixed length (1/2/3 hop to CVE or 2/3/4 hop to Mitigation), and conjunct the sampled paths together by the CVE entity. We randomly remove half of the facts from KG that exists in the evaluation set, which addresses the assumption of incomplete KG hence relies on the reasoning to find correct answers.

DRKG – We directly use a constructed drug repurposing KG. Table 15 shows the overall statistics of entity/relation/fact scales; we also add the reverse facts into DRKG.

Entity category	Data Source	Quantity
Vulnerability (CVE)	Webpage, BRON, NVD	18,587
Vendor	Webpage	2,223
Product	Webpage	7,103
Version	Webpage	96,725
Campaign	Webpage	13
Tactic	BRON	11
Technique	BRON	99
Attack pattern	BRON	323
Weakness (CWE)	Webpage, BRON	150
Mitigation	NVD	74,794
Total		200,028

Knowledge fact ($v \xrightarrow{r} v'$)	Quantity
Vendor $\xrightarrow{\text{develops}}$ Product	7,897
Product $\xrightarrow{\text{obtains}}$ Version	96,725
Vendor $\xrightarrow{\text{vulnerable to}}$ CVE	26,884
Product $\xrightarrow{\text{vulnerable to}}$ CVE	47,419
Version $\xrightarrow{\text{vulnerable to}}$ CVE	510,781
CVE $\xrightarrow{\text{aims to}}$ Campaign	27,325
CVE $\xrightarrow{\text{is related to}}$ CVE	2502
Tactic $\xrightarrow{\text{includes}}$ Technique	123
Technique $\xrightarrow{\text{leverages}}$ Attackpattern	111
Attackpattern $\xrightarrow{\text{applies to}}$ Weakness	575
Weakness $\xrightarrow{\text{contains}}$ CVE	19,047
CVE $\xrightarrow{\text{fixable by}}$ Mitigation	125,943
Total (w. reverse facts)	1,730,664

Table 14. Statistics of cyber-domain KG.

# Entity	# Relation	# Fact (w. reverse)
97,238	107	11,748,522

Table 15. Statistics of DRKG.

D Parameter Setting

Table 16 summarizes the default parameter setting used in §5 and §6.

E Additional Results

Figure 14 shows the MRR variation before and after attacks with respect to n_{kp} and n_{qp} . The observations are similar to Figure 5.

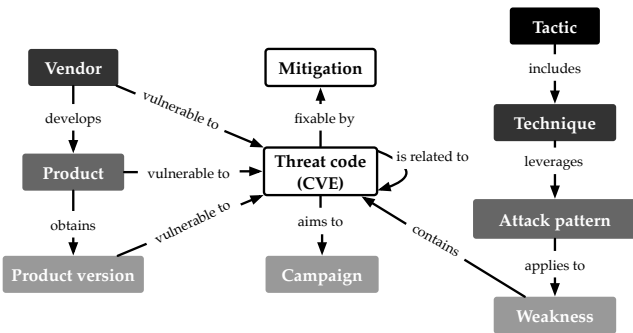


Figure 11: Structure of our cyber-domain knowledge graph.

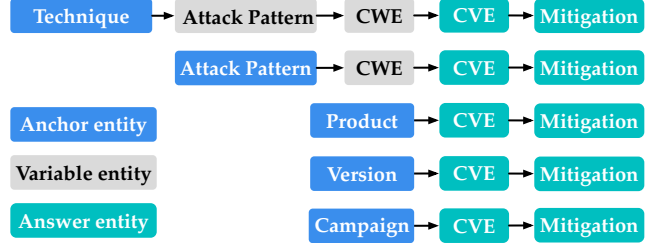


Figure 12: Different logical paths used in our query set.

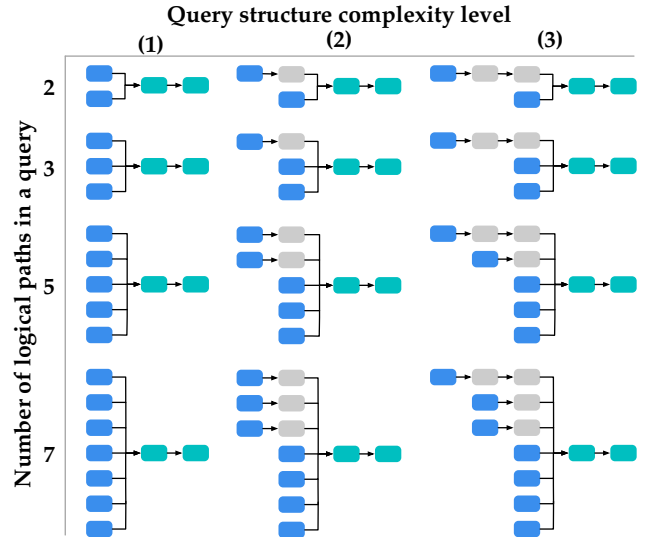


Figure 13: Topological structures of queries used in cyber-threat hunting (blue – anchor; grey – variable; green – answer).

Type	Parameter	Setting
Cyber-Threat Hunting		
Encoder ϕ	Dimension	400
Operator ψ	Query2Box Architecture	2FC (Projection)
	Hidden Dim	2FC (Conjunction)
Training	Learning rate	0.001 (ϕ and γ)
	Batch size	512 (ϕ and γ)
	Epochs	80000 (ϕ), 10000 (γ)
	Optimizer	Adam (ϕ and γ)
Attack	n_{kp}	100
	n_{qp}	2
	n_{iter}	5
Drug Repurposing		
Encoder ϕ	Dimension	200
Operator ψ	R-GCN Architecture	2GraphConv
	Hidden Dim	200
Training	Learning rate	0.0001 (ϕ), 0.001 (γ)
	Batch size	2048 (ϕ and γ)
	Epochs	100000 (ϕ), 20000 (γ)
	Optimizer	Adam (ϕ and γ)
Attack	n_{kp}	400
	n_{qp}	20
	n_{iter}	5

Table 16. Default parameter setting.

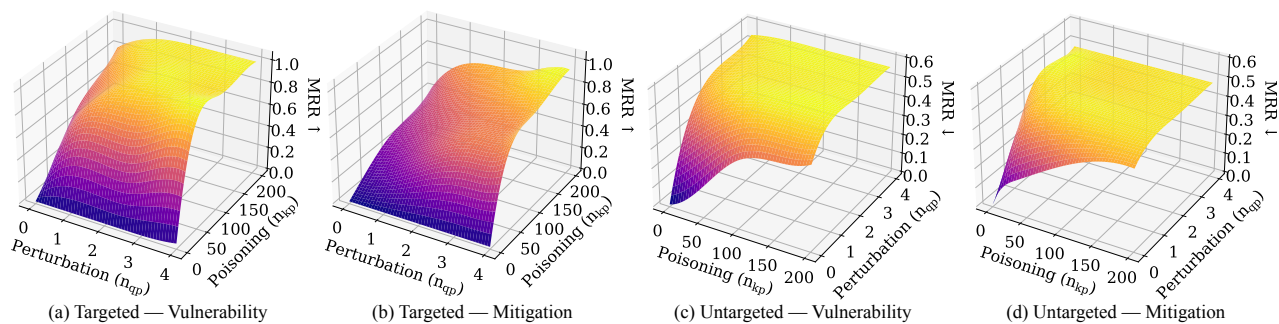


Figure 14: MRR variation of ROAR_{CO} with respect to knowledge poisoning budget (n_{kp}) and query perturbation budget (n_{qp}).